

High Frequency Finance: Using Scaling Laws to Build Trading Models

ALEXANDRE DUPUIS and RICHARD B. OLSEN
Olsen Ltd., University of Essex

20.1 Introduction

The availability of large amounts of tick-by-tick data, in excess of 50,000 data points per day (Glattfelder et al., 2010), oanda, ebs has opened up new opportunities for model building. It is now possible to follow an empirical approach and develop models bottom up by analyzing empirical data and searching for statistical properties.

The analysis of high frequency data is nontrivial: ticks (i.e., quoted prices) are irregularly spaced in time in an intricate sequence. The available literature essentially suggests two ways to handle this issue (Dacorogna et al., 2001; Engle and Russell, 2006). The first method suggests aggregating price information by interpolating prices between fixed and predetermined times. The drawback of this method is the loss of intratime information during active periods and the multiplication of price information during quiet periods, when insufficient data is available. With the second approach, one can consider a time series made of ticks and times between their occurrences (i.e., duration); this is referred to as a *point process* (Bauwens and Hautsch, 2009). Point processes are valuable because they incorporate durations and allow analytical results to be derived; however, they have the disadvantage that time is measured in terms of physical units, and therefore, point processes neither adapt to the changing market activity nor

differentiate between a minute of early morning calm and a minute during a hectic news announcement.

We propose a different way to analyze high frequency data: an event-based approach in which the time series is dissected based on market events where the direction of the trend changes from up to down or vice versa. We identify alternating directional changes (DCs) as a price move of magnitude λ from the last price extreme, be it a high or a low when a downward or upward directional change is to be observed, respectively (Guillaume et al., 1997). Physical time is substituted with the so-called intrinsic time incremented by one unit whenever a directional change occurs. This approach is well suited to deal with tick-by-tick data because it is not constrained by any fixed time grid and naturally adapts to the market activity. With this methodology, we can model the price curve as a superposition of different λ price curves based on directional changes.

We have discovered 12 new scaling laws (Glattfelder et al., 2010) that researchers had failed to previously identify. The scaling laws are powerful tools for model building: they are a frame of reference to relate different values to each other. We use the scaling laws to compute the equivalent of a Richter scale in geology (Richter, 1958) for financial markets. The scale of market quakes (SMQ, Bisig et al., 2012) is an objective measure of the impact of political and economic events in foreign exchange and used as a support tool for decision makers and commentators in financial markets or as an input for an economic model measuring the impact of fundamental economic events.

The discovery of the 12 new scaling laws can be used as a cornerstone for model building. They provide a dynamic frame of reference, which is a kind of anchor for the rest of the model. One of the scaling laws relates the total length of the coastline of the price curve as a function of the threshold of observation. If we sum up all the price changes bigger or equal to 0.05% after subtracting potential transaction costs, then the 1-year coastline is an astounding 1600% compared to a price risk of 30%. The length of the coastline is the result of the ongoing imbalance between buyers and sellers and reflects a lack of market liquidity, when there are not enough market participants ready to take the other side of the immediate buy or sell flow.

We have developed a new class of trading models that is based on the scaling law of price overshoots. The algorithm opens countertrend positions, when there is an imbalance of buy and sell volume and a price overshoot occurs. The position is closed out as soon as the position is back in a profit. The model takes advantage of the long coastline and the recurring price rebounds and improves the price average of the position by adding and subtracting to the position during the temporary rebounds and generating incremental return that speeds up the time for the closing of the position. Besides generating return, the strategy provides liquidity to the market and reduces its overall volatility; this has economic value because it lowers uncertainty, thus increasing economic efficiency. The lack of correlation with other asset classes and investment strategies makes high frequency finance strategies an attractive new asset class with unique features: stable returns. An additional advantage is the liquidity of these strategies because investments can be closed out at any time.

The strategy can also be embedded as part of a dynamic currency overlay; in conjunction with a static hedge, the dynamic hedge generates incremental return and reduces overall risk: the dynamic hedge increases the size of its position, whenever the underlying asset appreciates too rapidly, and starts to offset the static hedge by building up long positions, whenever the asset drops too rapidly. The incremental returns of the dynamic component turn currency hedging into an attractive financial product.

The chapter is organized as follows. In Section 20.2, we define the event-based framework in some detail. The scaling laws are then presented in Section 20.3. Section 20.4 introduces the SMQ and analyzes SMQ events during the course of several years for major currency pairs. The main features of our trading model algorithm are then described in Section 20.5, where we discuss monthly statistics of executed trades. Finally, we conclude and discuss further work.

20.2 The Intrinsic Time Framework

The foreign exchange (FX) market is usually analyzed as a homogeneous sequence of returns r defined as the price difference over a fixed period of time (Dacorogna et al., 2001). This metric is used for a discontinuous time series: over weekends, trading comes to a standstill or, inversely, at news announcements, there are spurts of market activity. Ideally, time should be a dynamic object that adapts itself to market activity. To achieve this goal, we propose an event-based approach that analyzes the time series in terms of price directional changes of a given amplitude λ (Glattfelder et al., 2010). Within this framework, time flows unevenly: any occurrence of a directional change represents a new *intrinsic* time unit. Intrinsic time flows to the beat of events and is thus better suited to model the dynamics of the underlying processes.

The dissection algorithm identifies the occurrence of a price change λ from the last high or low (i.e., an extrema), whether it is in an up or down mode, respectively. At each occurrence of a directional change, there is the so-called overshoot associated with the previous directional change. The overshoot is defined as the difference between the price level at which the last directional change occurred and the extrema before the next directional change is triggered. Figure 20.1 shows how the price curve is dissected into directional change and overshoot sections.

Formally, we map the time series of prices into sequences of directional changes and price overshoots as follows. Let $\Lambda = \{\lambda_0, \dots, \lambda_{m_\lambda-1}\}$ be the set of n_λ price thresholds onto which time series is mapped. The initial condition of the sequence is x_0 , the initial price; t_0 , the initial physical time; and m_0 , the mode that switches between up and down indicating in which direction the directional change is expected. An initial condition affects at most the first two pairs (directional change, overshoot), and let the subsequent pairs in the sequence to synchronize with any other sequence obtained with a different initialization.

A given λ_j discretizes the time series into a set of prices $X_j(t) = \{x_0^j(t_0^j), \dots, x_{n_j-1}^j(t_{n_j-1}^j), x(t)\}$ occurring at times $T_j(t) = \{t_0^j, \dots, t_{n_j-1}^j, t\}$, where $x(t) =$

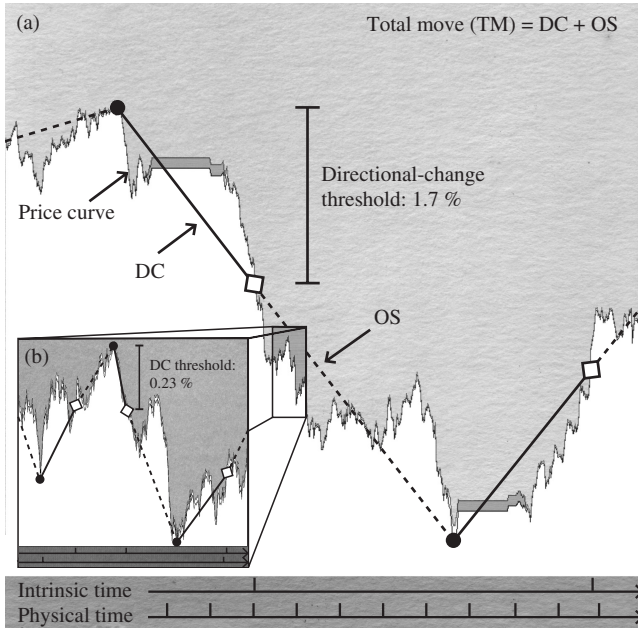


FIGURE 20.1 Projection of a (a) 2-week, (b) zoomed-in 36-h price sample onto a reduced set of the so-called directional-change (DC) events defined by a threshold (a) $\lambda = 1.7\%$, (b) $\lambda = 0.23\%$. These DC events (diamonds) act as natural dissection points, decomposing a total-price move between two extremal price levels (bullets) into the so-called DC (solid lines) and overshoot (OS, dashed lines) sections. Timescales depict physical time ticking evenly across different price-curve activity regimes, whereas *intrinsic time* triggers only at DC events.

$(bid(t) + ask(t))/2$ is the midprice at time t . We highlight that the last elements of the set $(x(t), t)$ are temporary, as they do not correspond to a turning point yet but represent the state of the process at time t . We compute the number of turning points (i.e., the occurrence of a directional change) as $n_e^i = \lfloor n_i/2 \rfloor$. The series of amplitude of directional changes Δ_i is defined as

$$\Delta_i(t) = \left\{ \delta_0^i, \dots, \delta_{n_e^i-1}^i, \delta_{n_e^i}^i(t) \right\} = \left\{ \frac{x_{2j+1}^i - x_{2j}^i}{x_{2j}^i} \right\} \quad (20.1)$$

where $0 \leq j \leq n_e^i$. The discreteness of the time series of prices prevents $|\delta_j^i| = \lambda_i$. The discrepancy is, however, small and is on average within the spread. The series of amplitudes of overshoots Ω_i is written as

$$\Omega_i(t) = \left\{ \omega_0^i, \dots, \omega_{n_e^i-1}^i, \omega_{n_e^i}^i(t) \right\} = \left\{ \frac{x_{2(j+1)}^i - x_{2j+1}^i}{x_{2j+1}^i} \right\} \quad (20.2)$$

Durations of directional changes or price overshoots are similarly defined by replacing prices x by physical time t in Equations (20.1) and (20.2).

Algorithm 20.1 shows a pseudocode that gives further details on how to dissect the time series of prices.

ALGORITHM 20.1 Dissect the price curve from time t_0 and measure overshoots with a λ_i price threshold

Require: initialise variables ($x^{\text{ext}} = x(t_0)$, *mode* is arbitrarily set to *up*, $X_i = x_0$, $T_i = t_0$)

```

1: update latest  $X_i$  with  $x(t)$ 
2: update latest  $T_i$  with  $t$ 
3: if mode is down then
4:   if  $x(t) > x^{\text{ext}}$  then
5:      $x^{\text{ext}} \leftarrow x(t)$ 
6:   else if  $(x^{\text{ext}} - x(t))/x^{\text{ext}} \geq \lambda_i$  then
7:      $x^{\text{ext}} \leftarrow x(t)$ 
8:     mode  $\leftarrow$  up
9:      $X_i \leftarrow x(t)$ 
10:     $T_i \leftarrow t$ 
11:   end if
12: else if mode is up then
13:   if  $x(t) < x^{\text{ext}}$  then
14:      $x^{\text{ext}} \leftarrow x(t)$ 
15:   else if  $(x(t) - x^{\text{ext}})/x^{\text{ext}} \geq \lambda_i$  then
16:      $x^{\text{ext}} \leftarrow x(t)$ 
17:     mode  $\leftarrow$  down
18:      $X_i \leftarrow x(t)$ 
19:      $T_i \leftarrow t$ 
20:   end if
21: end if

```

Section 20.3 explores the relationships between the quantities introduced above and empirically shows that a large number of scaling laws exist. We then introduce a novel way to measure market activity by inspecting the behavior of an aggregate of $\omega_{n_i}^i(t)$ over i on a continuous basis.

20.3 Scaling Laws

Scaling laws establish invariance of scale and play an important role in describing complex systems (Barabasi and Albert, 1999; Newman, 2005; West et al., 1997). In finance, there is one scaling law that has been widely reported (Balocchi et al., 1999; Corsi et al., 2001; Dacorogna et al., 2001; Di Matteo et al., 2005; Galluccio et al., 1997; Mantegna and Stanley, 1995; Müller et al., 1990; Guillaume et al., 1997): the size of the average absolute price change (return) is

scale-invariant to the time interval of its occurrence. This scaling law has been applied to risk management and volatility modeling (Di Matteo, 2007; Gabaix et al., 2003; Ghashghaie et al., 1996; Sornette, 2000), even though there has been no consensus among researchers for why the scaling law exists (Barndorff-Nielsen and Prause, 2001; Bouchaud, 2001; Farmer and Lillo, 2004; Joulin et al., 2008; Lux, 2006).

Searching for new scaling laws, we analyze the price data of the FX market, which is a complex network of interacting agents: corporations, institutional and retail traders, and brokers trading through market makers, who themselves form an intricate web of interdependence. We consider five years of tick-by-tick data for 13 exchange rates through November 2007 (see Glattfelder et al. (2010) for a description of the data set).

An exchange rate often moves by 10–20% within a year. However, since the seminal work of Mandelbrot (1963), we know about the fractal nature of price curves. The coastline, roughly being the sum of all price moves of a given threshold, at fine levels of resolution, may be far longer than one might intuitively think. But how much longer? The scaling laws described in this chapter provide a surprisingly accurate estimate and not only highlight the importance of considering tail events (Sornette, 2002) but also set these in perspective with the remarkably long coastline of price changes preceding them.

20.3.1 THE NEW SCALING LAWS

Interest in scaling relations in FX data was sparked in 1990 by a seminal paper relating the mean absolute change of the logarithmic midprices, sampled at time intervals Δt over a sample of size $n\Delta t$, to the size of the time interval (Müller et al., 1990)

$$\langle |\Delta \chi| \rangle_p = \left(\frac{\Delta t}{C_\chi(p)} \right)^{E_\chi(p)} \quad (20.3)$$

where $\Delta \chi_i = \chi_i - \chi_{i-1}$ and $\chi_i = \chi(t_i) = (\ln \text{bid}_i + \ln \text{ask}_i)/2$ is the logarithmic midprice of a currency pair at time t_i , and $E_\chi(p)$, $C_\chi(p)$ are the scaling-law parameters. The averaging operator is $\langle x \rangle_p = (1/n \sum_{j=1}^n x_j^p)^{1/p}$, usually with $p \in \{1, 2\}$, and p is omitted if equal to one. Note that for law (20.3), the data is sampled at fixed time intervals $t_i = i\Delta t$. This requires a time interpolation scheme (described in Glattfelder et al. (2010)), which we will also employ when necessary. Throughout the chapter, we consider a simpler definition of the price given by $x_i = (\text{bid}_i + \text{ask}_i)/2$, where price moves are defined as $\Delta x_i = (x_i - x_{i-1})/x_{i-1}$. Although the definition of x_i loses the mathematical feature of χ_i of behaving antisymmetrically under price inversions (e.g., $\chi_i^{\text{EUR-USD}} = -\chi_i^{\text{USD-EUR}}$), it is more natural because, practically, percentages are more intuitive to manipulate than differences between logarithmic values. However, considering either χ_i or x_i leads to very similar results even for large spread values.

Later, in 1997, a second scaling law was reported by Guillaume et al. (1997), relating the number $N(\Delta\chi_{dc})$ of directional changes to the directional-change sizes $\Delta\chi_{dc}$

$$N(\Delta\chi_{dc}) = \left(\frac{\Delta\chi_{dc}}{C_{N,dc}} \right)^{E_{N,dc}}. \quad (20.4)$$

In Glattfelder et al. (2010), and reviewed here, we confirm laws (20.3) and (20.4), considering x_i (Fig. 20.3a–c), and report on 12 new independent scaling laws holding across 13 exchange rates and for close to three orders of magnitude. Tables of the estimated parameter values for all the laws and for the 13 exchange rates, as well as for a Gaussian random walk (GRW) model, are provided in Glattfelder et al. (2010). Table 20.1 shows the estimated scaling-law parameters for EUR-USD. We start the enumeration of the laws by a generalization of Equation (20.4) that relates the average number of ticks observed during a price move of Δx to the size of this threshold

$$\langle N(\Delta x_{\text{tick}}) \rangle = \left(\frac{\Delta x}{C_{N,\text{tick}}} \right)^{E_{N,\text{tick}}} \quad (20.5)$$

where a tick is defined as a price move larger than (in absolute value) $\Delta x_{\text{tick}} = 0.02\%$. The definition of a tick can, however, be altered without destroying

TABLE 20.1 Estimated Scaling-Law Parameter Values Considering EUR-USD

Name	Equation	E	C
Tick count	20.5	1.93	2.1×10^{-2}
Price move count	20.6	-1.93	9.5×10^0
Maximum price move	20.7 ($p = 1$)	0.52	1.9×10^5
Maximum price move	20.7 ($p = 2$)	0.49	1.3×10^5
Time of price move	20.8	1.93	1.2×10^{-3}
Time of directional change	20.9	1.88	1.1×10^{-3}
Total-price move	20.13	0.98	4.9×10^{-1}
Overshoot move	20.13	1.0	9.9×10^{-1}
Time of total move	20.16	1.89	1.1×10^{-3}
Time of directional change	20.16	1.85	1.6×10^{-3}
Time of overshoot	20.16	1.91	1.4×10^{-3}
Total-move tick count	20.17	1.89	1.9×10^{-2}
Directional-change tick count	20.17	2.02	4.2×10^{-2}
Overshoot tick count	20.17	1.87	2.3×10^{-2}
Cumulative total move	20.18	-0.94	2.0×10^2
Cumulative total move with costs	20.18	-0.98	1.5×10^2
Cumulative directional change	20.18	-0.95	8.8×10^1
Cumulative overshoot	20.18	-0.92	1.1×10^2

the scaling-law relation. In essence, this law counts the average number of ticks observed during every price move Δx . Law (20.5) is plotted in Figure 20.2. The second law counts the average yearly number $N(\Delta x)$ of price moves of size Δx

$$N(\Delta x) = \left(\frac{\Delta x}{C_{N,x}} \right)^{E_{N,x}} \tag{20.6}$$

We annualize the number of observations of laws (20.4) and (20.6) by dividing them by 5, the number of years in our data sample. Law (20.6) and all the following scaling laws are given in Figure 20.3 The next scaling law relates the average maximal price range Δx_{\max} , defined as the difference between the high and low price levels, during a time interval Δt , to the size of that time interval

$$\langle \Delta x_{\max} \rangle_p = \left(\frac{\Delta t}{C_{\max}(p)} \right)^{E_{\max}(p)} \tag{20.7}$$

Tick-count scaling law

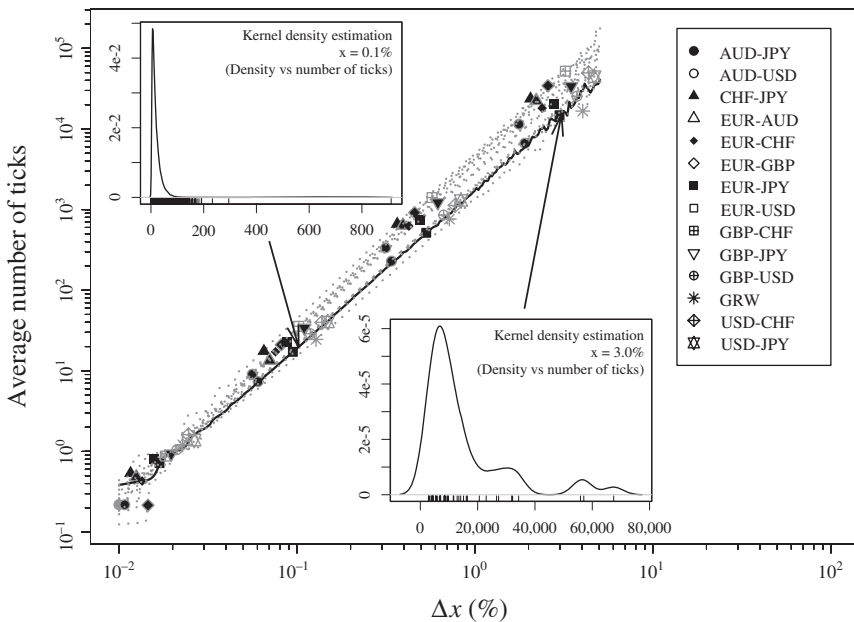


FIGURE 20.2 Scaling law (20.5) is plotted, where the x -axis shows the price move thresholds of the observations and the y -axis, the average tick numbers. A tick is defined as a price move of 0.02%. The solid line shows the raw data for EUR-USD. For the remaining 12 currency pairs and the Gaussian random walk benchmark model, the raw data is displayed with dots. Insets show the distribution of the EUR-USD observations (drawn above their x -axis) for selected threshold values of 0.1% and 3.0%. See Glattfelder et al. (2010) for the values of the estimated scaling-law parameters.

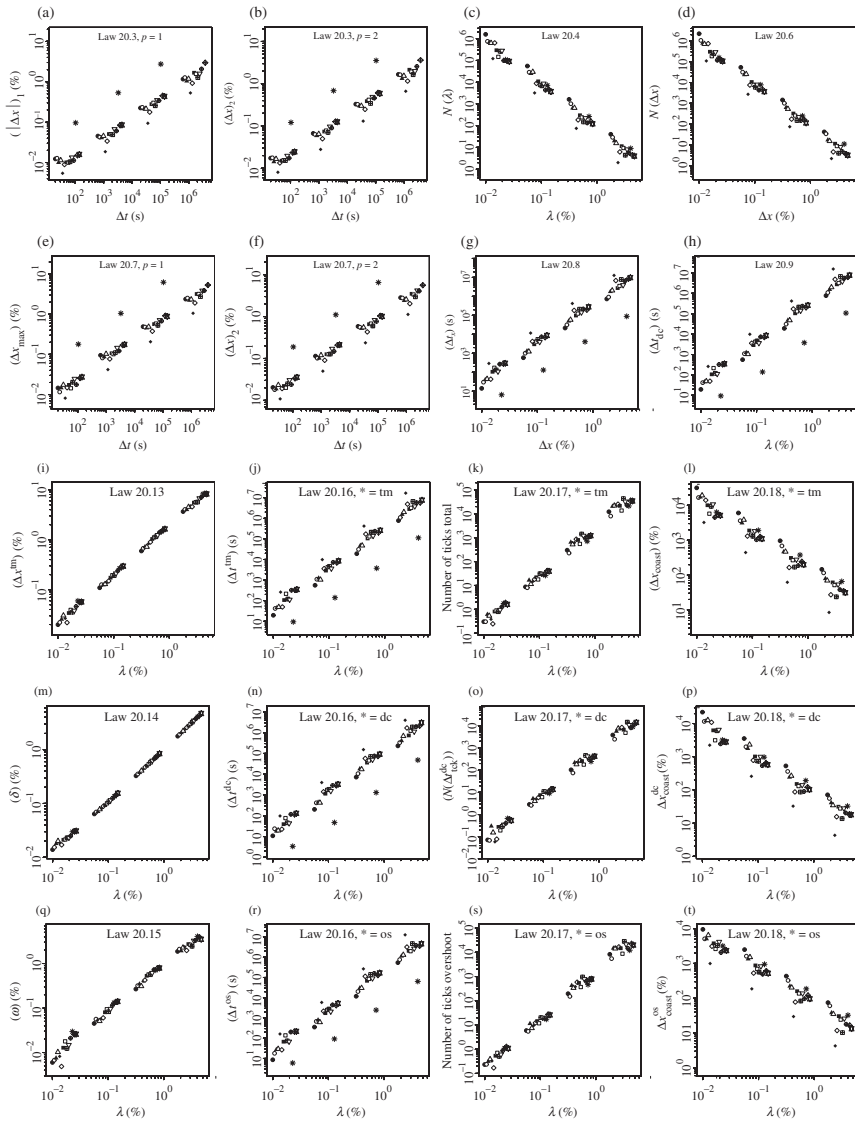


FIGURE 20.3 Plots of all scaling laws described in the text. (a) Mean price move, (b) quadratic mean price move, (c) directional-change count, (d) price move count, (e) maximum price move, (f) quadratic mean maximum price move, (g) mean time of price move, (h) time during directional changes, (i) total-price move, (j) time of total move, (k) total-move tick count, (l) coastline (cumulative total move), (m) directional-change move, (n) time of directional change, (o) directional-change tick count, (p) cumulative directional change, (q) overshoot move, (r) time of overshoot, (s) overshoot tick count, and (t) cumulative overshoot. Symbols are as in Figure 20.2. The raw data is plotted for the 13 currency pairs with dots and for the Gaussian random walk model with dashes. See Glattfelder et al. (2010) for the values of the estimated scaling-law parameters.

where $\Delta x_{\max} = \max\{x(\tau); \tau \in [t - \Delta t; t]\} - \min\{x(\tau); \tau \in [t - \Delta t; t]\}$ and Equation (20.7) holds for $p = 1, 2$.

The statistical properties of a GRW are, as is well known, different to the observed empirical data in many respects (Mandelbrot and Hudson, 2004). Having said this, it is striking how closely this simple model can reproduce many of the average statistical properties of the real market. Notable differences are seen in law (20.7) (Figs 20.3e and f), which reveal an unintuitive result: the bell-curve distribution of price moves leads to an average maximal price move that is roughly eight times larger than that observed for the empirical data.

We have also discovered laws relating the time during which events happen to the magnitude of these events. Law (20.8) relates the average time interval $\langle \Delta t_x \rangle$ for a price change of size Δx to occur to the size of the threshold

$$\langle \Delta t_x \rangle = \left(\frac{\Delta x}{C_{t,x}} \right)^{E_{t,x}} \quad (20.8)$$

and similarly, considering directional changes of threshold λ

$$\langle \Delta t_{dc} \rangle = \left(\frac{\lambda}{C_{t,dc}} \right)^{E_{t,dc}} \quad (20.9)$$

Thus, laws (20.8) and (20.9) relate the average numbers of seconds that elapse between consecutive price moves and directional changes, respectively.

Next, we unveil a set of scaling laws emerging from the identification of directional-change events that make up the so-called total-move (TM) segments, which themselves decompose into directional-change (DC) and overshoot (OS) parts. The total-price move, waiting time, and number of ticks can then be written as

$$\langle |\Delta x^{\text{tm}}| \rangle = \langle |\delta| \rangle + \langle |\omega| \rangle, \quad (20.10)$$

$$\langle \Delta t^{\text{tm}} \rangle = \langle \Delta t^{\text{dc}} \rangle + \langle \Delta t^{\text{os}} \rangle, \quad (20.11)$$

$$\langle N(\Delta x_{\text{tck}}^{\text{tm}}) \rangle = \langle N(\Delta x_{\text{tck}}^{\text{dc}}) \rangle + \langle N(\Delta x_{\text{tck}}^{\text{os}}) \rangle. \quad (20.12)$$

This decomposition leads to nine additional scaling laws, where the average values are functions of the directional-change thresholds λ

$$\langle |\Delta x^{\text{tm}}| \rangle = \left(\frac{\lambda}{C_{x,\text{tm}}} \right)^{E_{x,\text{tm}}} \quad (20.13)$$

$$\langle |\delta| \rangle = \left(\frac{\lambda}{C_{x,dc}} \right)^{E_{x,dc}} \quad (20.14)$$

$$\langle |\omega| \rangle = \left(\frac{\lambda}{C_{x,os}} \right)^{E_{x,os}} \quad (20.15)$$

$$\langle \Delta t^* \rangle = \left(\frac{\lambda}{C_{t,*}} \right)^{E_{t,*}} \quad (20.16)$$

$$\langle N(\Delta x_{\text{tick}}^*) \rangle = \left(\frac{\lambda}{C_{N,*}} \right)^{E_{N,*}} \quad (20.17)$$

where $*$ stands for {tm, dc, os}. Note that $\langle |\delta| \rangle = \lambda$ holds by construction. The actual deviation to $E_{x,\text{dc}} = 1$ and $C_{x,\text{dc}} = 1$, as seen in Glattfelder et al. (2010), is given by the increasing noise for small thresholds, as the impact of the effect of a tick exceeding the exact threshold systematically overestimates $\langle |\delta| \rangle$ (Fig. 20.3m). The average parameter values (across the 13 currency pairs) of law (20.13) display a peculiar feature: on average, a directional change λ is followed by an overshoot of the same magnitude $\langle |\omega| \rangle \approx \lambda$ ($E_{x,\text{os}}^{\text{av}} \approx 1.04$ and $C_{x,\text{os}}^{\text{av}} \approx 1.06$), making the total move double the size of the directional-change threshold $\langle |\Delta x^{\text{tm}}| \rangle \approx 2\lambda$ ($E_{x,\text{to}}^{\text{av}} \approx 0.99$ and $C_{x,\text{to}}^{\text{av}} \approx 0.51$). This result is also found by computing the probable path of the price within a binomial tree as $0.5\Delta x + 0.5^2 2\Delta x + 0.5^3 3\Delta x + \dots = \Delta x \sum_{i=1}^n i 0.5^i \xrightarrow{n \rightarrow \infty} 2\Delta x$. A similar feature holds for the waiting times and number of ticks: $\langle |\Delta t^{\text{os}}| \rangle \approx 2\langle |\Delta t^{\text{dc}}| \rangle$ and $\langle N(\Delta x_{\text{tick}}^{\text{os}}) \rangle \approx 2\langle N(\Delta x_{\text{tick}}^{\text{dc}}) \rangle$. Although in terms of size the overshoot price move is approximately as big as the direction-change threshold, it contains roughly twice as many ticks and takes twice as long to unfold.

Considering cumulative price moves instead of the averages in law (20.3) leads to another triplet of laws

$$\Delta x_{\text{cum}}^* = \sum_{i=1}^n |\Delta x_i^*| = \left(\frac{\lambda}{C_{\text{cum},*}} \right)^{E_{\text{cum},*}} \quad (20.18)$$

This concludes the presentation of 17 new scaling laws: we count Equation (20.7) twice for $p = 1, 2$ and omit the trivial scaling law $\langle |\delta| \rangle \propto \lambda$. In Glattfelder et al. (2010), we actually show that 12 laws are independent and hence can be understood as primary laws.

20.3.2 THE COASTLINE

We now have the necessary tools in hand to come back to the measurement of the length of the coastline. The total-move scaling law (20.18) allows us to estimate its size as a function of the resolution defined by the directional-change threshold. Considering thresholds of 0.01%, 0.1%, 1%, and 5%, one finds the average lengths of the annualized coastline to be 22, 509%, 2046%, 186%, and 34.8%, respectively. So by decreasing the threshold of resolution 500-fold, the length of the coastline decreases by a factor of 650. Similarly, looking at the GRW, we find 14, 361%, 1946%, 264%, and 65.2%, respectively. The 500-fold decrease in resolution entails a coastline decrease by a factor of only 220, highlighting the fact that GRW has fewer small moves and more middle-sized moves than the empirical price curves. Not surprisingly, taking transaction

costs into account breaks the scaling law for small thresholds. However, it is still possible to evaluate the length of the coastline by employing the scaling relation for the interval [0.1%, 5%] and measuring it for 0.05%. Thus, for the thresholds 0.05%, 0.1%, 1%, and 5% the new average coastline lengths are now 1, 604%, 1, 463%, 161%, 34.5%. For the 0.05% threshold (which occurs on average every 15 min), we measure an average daily coastline of 6.4%. The range of these average daily coastline lengths is from 1.8% for EUR-CHF to 9.1% for AUD-JPY.

20.4 The Scale of Market Quakes

Scaling laws relate price moves, duration, and frequency; let us use this scaling-law methodology to measure multiscale events such as market responses due to news announcements or price jumps due to endogenous factors, such as lack of liquidity (Joulin et al., 2008). Although a considerable amount of research has been devoted to quantifying market impact of such events, see for example Bauwens et al. (2005), Bouchaud (2009), Chaboud et al. (2004), Dominguez (2003), Engle and Ng (1993) and references therein, there has been to our knowledge only one attempt at quantifying multiscale events (Zumbach, 2000) where the authors propose a scale that is a weighted average of returns over different (physical) time horizons. This approach suffers from the rigidity of physical time and does not seem to measure comparable magnitudes over different currency pairs. To alleviate these issues, and also inspired by the Richter scale Richter (1958), we propose a methodology to quantify these multiscale events along a scale, the SMQ (Bisig et al., 2012), which defines a tick-by-tick metric allowing us to quantify market quakes on a continuous basis where we monitor the excess price moves from one directional change to the next, that is, the price overshoots. In the rest of this section, we summarize the main findings from Bisig et al. (2012).

The SMQ can be used in different ways; decision makers can use the indicator as a tool to filter the significance of market events. The output of the SMQ can be used as an input to forecasting or trading models to identify regime shifts and change the input factors.

Every occurrence of a directional change triggers a new overshoot that oscillates between $-\lambda$ and any positive value until it decreases by $-\lambda$ from its recent price extreme causing the next directional change. Figure 20.4(a) shows the overshoot dynamics.

To measure the market activity over a range of price scales, we define an average overshoot $\bar{\omega}$ as

$$\bar{\omega}(t) = \frac{1}{n_\lambda} \sum_{i=1}^{n_\lambda} \omega^q(t, \lambda_i) \quad (20.19)$$

where n_λ is the number of thresholds λ_i and the superscript q denotes the quantile taken from the historical distribution of price overshoot associated to a

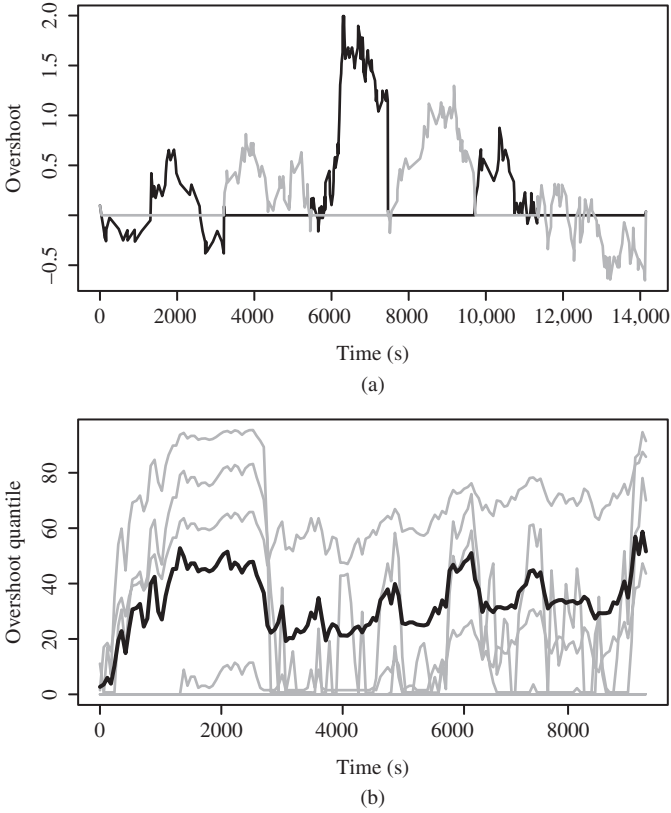


FIGURE 20.4 Sample evolution of (a) the price overshoot $\omega(t)$ and (b) the average price overshoot $\bar{\omega}(t)$. (a) Alternated gray and black lines show the overshoot normalized by λ . (b) A subset of the n_λ thresholds are shown in gray and the black line shows the average overshoot $\bar{\omega}(t)$. Overshoots are measured in quantiles to ensure a normalized measurement.

threshold λ and computed from tick-by-tick date from December 1, 2005, up to December 31, 2008. Overshoots are expressed in quantiles to ensure a normalized measurement and to be averaged over different thresholds. We consider evenly distributed thresholds and set $\lambda_i = i \cdot 0.05\%$ with i running from 1 to $n_\lambda = 100$. Figure 20.4(b) shows the time evolution of $\bar{\omega}$.

We now describe the way the average overshoot $\bar{\omega}(t)$ is converted into a unique number: the SMQ $\mathcal{S}(t)$. It is defined as

$$\mathcal{S}(t) = \frac{1}{n_a} \sum_{i=0}^{n_a} \mathcal{F} \left(\bar{\Omega} \left(t + \left(\frac{2i}{n_a} - 1 \right) \delta t \right) \right) \tag{20.20}$$

where δt is the time window, $n_a = \delta t / \delta t_a$ is the time discretization of the average and the set $\bar{\Omega}(t) = \{\bar{\omega}(\tau) - \langle \bar{\omega}(\tau) \rangle_{\bar{\Omega}(t)} | t - \delta t \leq \tau \leq t + \delta t\}$. The average operator $\langle \cdot \rangle_{\bar{\Omega}(t)}$ is used to prevent high or low plateaux to correspond to significantly

different frequencies. The operator $\mathcal{F}(\cdot)$ is defined as

$$\mathcal{F}(\bar{\Omega}(t)) = \frac{1}{\lfloor n_f/2 + 1 \rfloor} \sum_{k=1}^{\lfloor n_f/2 + 1 \rfloor} \frac{|X_{k-1}|}{k} \quad (20.21)$$

where $n_f = \delta t / \delta t_f$ is the time discretisation of $\bar{\Omega}(t)$, $\lfloor \cdot \rfloor$ is the floor operator, and $|X_k|$ is the magnitude of the Fourier frequency computed from the discretized set $\Omega(t)$. The average is done only over half of the frequencies as the Fourier transform of a real signal is symmetric around the middle of the spectrum. The weighting ensures the robustness of the operator $\mathcal{F}(\cdot)$ to small perturbations.

Figure 20.5(a–h) shows the behavior of EUR-USD and the SMQ on the occasion of eight releases of nonfarm employment numbers Bureau of Labour Statistics. The wide variety of market responses: a steep drop (f), the same price move amplitude as in (f) but happening within a longer time period (e), little reaction from the market (c), volatile market (g and h), or a drop immediately followed by a recovery (b and g) is characterized by our methodology computing a single number within the SMQ. As expected, we observe that the steep drop (f) is associated with a higher value than (e), where the difference between the two scenarios is mainly the time for the price move to occur. Scenario (b), which could well go unnoticed as the original price level does not seem to be altered by the news announcement, is given a significant SMQ magnitude that is comparable to (e).

We also noticed in Figure 20.5a, b, and d that peaks of SMQ magnitude do not always coincide with releasing time, as the market response can take a few hours to operate.

As in the case of earthquakes, after-quakes occur, such as in (a and g), and have, in contrast to what is shown here, also been observed to be stronger than the original quake. The initial market impact can trigger margin calls that can trigger a far bigger secondary market shock.

Figure 20.5i shows the distribution of the SMQ magnitude of two sets of events versus the maximum price move that occurred within the next 12 hours following the events. The first events considered are 27 nonfarm employment change announcements between 2007 and 2009, and the second ones are 4687 SMQ magnitude peaks observed between December 2005 and March 2009, where a SMQ magnitude peak corresponds to a value $\mathcal{S}(t)$, where $\mathcal{S}(t) > \mathcal{S}(t \pm \delta t_a)$.

We observe a conelike structure where high values are not associated with any small price moves whereas large price moves can relate to small SMQ values. A high value necessarily implies that high price thresholds have been activated, but a noticeable price move can happen as a jump in the market and therefore does not necessarily correspond to a large SMQ value.

We stress here that we have opted for designing a scale that has a fixed frame of reference, implying that the average of observed SMQ magnitudes as well as their frequency can change over time, see Bisig et al. (2012) for analysis and discussion.

Here, we have restricted ourselves to EUR-USD and only considered US news. The same analysis can be done for other currency pairs and news events.

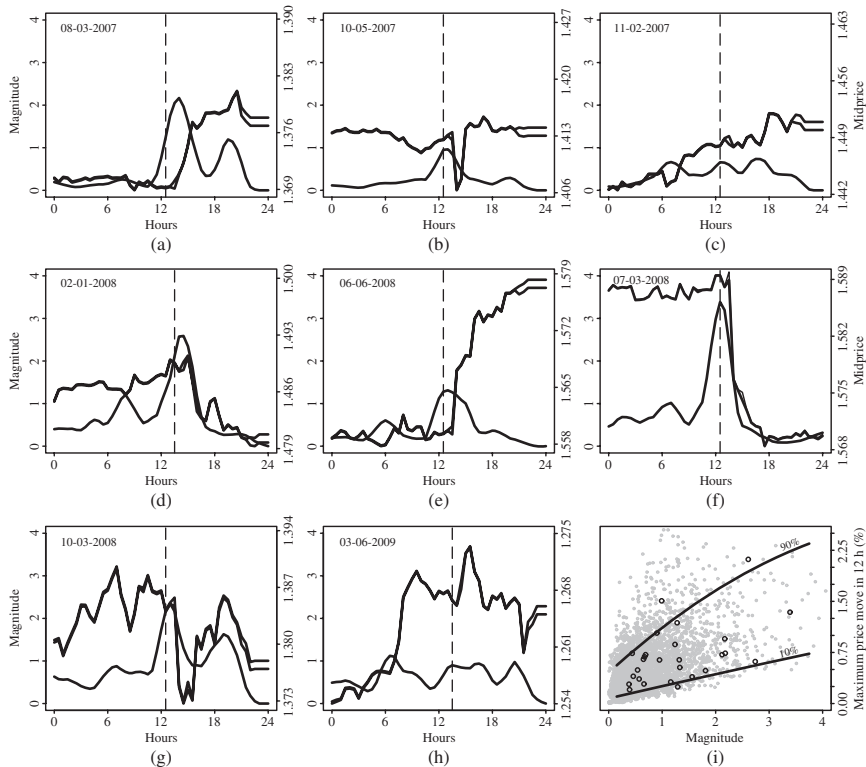


FIGURE 20.5 (a–h) Behavior of EUR-USD (thin lines) and the SMQ (thick line). The announcement time is the dashed line, and its date appears on the top left of the figure. (i) Distribution of the SMQ magnitude of two sets of events versus the maximum price move that occurred within the next 12 h following the events. The first events (black circles) are 27 nonfarm employment change announcements between 2007 and 2009, and the second ones (gray dots) are 4687 SMQ magnitude peaks observed between December 2005 and March 2009 where a SMQ magnitude peak $\mathcal{S}(t)$ is defined as $\mathcal{S}(t) > \mathcal{S}(t \pm \delta t_e)$. The 10% and 90% quantiles of the distribution are shown.

We are, as we write, applying this methodology to eight currencies and publish SMQ values for the main international news events at the www.olsen.ch.

20.5 Trading Models

20.5.1 OVERVIEW

In this section, we describe a new class of trading models. At Olsen, we use this type of trading model in a portfolio of more than 20 currency pairs. The positions of the trading models are countertrend, meaning that a price move down triggers a buy; a price up move, a sell. These models provide liquidity to

the market. Typically, prices move down when there is a lack of buyers, and they move up when there are not enough sellers. By being countertrend, we help balance demand and supply.

A trading model is made of basic agents: the so-called coastline traders that are described in some detail below. The strength of our models is the fact that these agents are identical across currency pairs. The only difference is the price scale λ at which they operate, which adapts to the changing volatility regimes.

20.5.2 COASTLINE TRADER

A coastline trader is a process that exploits profit opportunities contained in the long coastline of prices. As seen above, the coastline is made of the price moves up and down at a given price scale λ . As we shall see, trading the coastline generates profits that is used to improve the price average and speed up the closure of the position. On the price scale λ , the state of the process is defined by its exposure e_τ , price average a_τ , and the length of overshoot l_τ , where $\tau > 0$ is the age of the process expressed as the number of events. An event is the occurrence of a price move of size λ . We now describe the state variables and the way the process evolves.

A coastline trader is initialized when a price overshoot of magnitude ω is observed. A common choice is to set $\omega = 1 \cdot \lambda$ following the results shown above, stating that the average overshoot length is equal to the originating price move. Negative and positive price moves initialize long and short processes, respectively, with initial price average $a_0 = x_0$, where x_τ is the current bid or ask whether the process is short or long, respectively. The process has initially an exposure e_0 set to $G(l_0 = 0)$, where G is a function describing position increments. The quantity $l_\tau > 0, \forall \tau$ measures the price overshoot expressed as the number of λ price moves the process is in, from the current price to a_0 . Note that here the price overshoot does not end when an opposite λ price move occurs but when the process is, as we shall see, in a profit and closes itself.

The occurrence of a new $\pm\lambda$ price move respectively decreases or increases the counter l_τ and makes the process state to evolve. In case of an increase ($l_{\tau+1} = l_\tau + 1$), a trade of size $\Delta e_\tau = G(l_{\tau+1})$ is made and the exposure becomes

$$e_{\tau+1} = e_\tau + G(l_{\tau+1}) \quad (20.22)$$

The new trade improves the price average, which reads

$$a_{\tau+1} = \frac{a_\tau e_\tau + x_\tau G(l_{\tau+1})}{e_{\tau+1}} \quad (20.23)$$

where x_τ is the ask or bid price when the process is long or short, respectively.

On the other hand, when the length of the overshoot decreases by one unit ($l_{\tau+1} = l_{\tau} - 1$), part of the position $\Delta e_{\tau} = \gamma G(l_{\tau})$ is closed and the exposure becomes

$$e_{\tau+1} = e_{\tau} - \gamma G(l_{\tau}) \quad (20.24)$$

where $0 \leq \gamma \leq 1$ tunes the size of closing trades. The larger the γ , the more the coastline is traded as every up and down is fully traded. On the other hand, setting γ close to 1 usually implies that a stronger price recovery is needed for the process to be in a profit. We usually set $\gamma = 0.5$.

Closing part of the position generates a profit $\pi_{r,\tau}$ expressed as

$$\pi_{r,\tau} = \lambda^* \gamma G(l_{\tau}) x_{\text{bid},\tau} \quad (20.25)$$

where the price $x_{\text{bid},\tau}$ is the bid price at time τ (the bid is taken as the profit is positive) and where $\lambda^* \approx \lambda$ is the inner price move (i.e., where the spread has been deducted) that just occurred. Giving the discreteness of the time series of prices, λ^* is close to λ but usually not equal.

Because a profit is taken, the price average after having taken profit worsens and becomes

$$a_{\tau+1} = \frac{(a_{\tau} - \bar{x}_{\tau})e_{\tau} - \pi_{r,\tau}}{e_{\tau+1}} + \bar{x}_{\tau} \quad (20.26)$$

where \bar{x}_{τ} is the bid or the ask prices when the process is long or short, respectively.

We use the total realized profit $\pi_r = \sum \pi_{r,\tau}$ to improve the price average of the position. The coastline is thus used as a tool to manage positions. For that, we introduce an altered price average, the so-called realized average a_{τ}^r , that takes the total realized profit π^r into account

$$a_{\tau}^r = \frac{(a_{\tau} - \bar{x}_{\tau})e_{\tau} + \pi_r}{e_{\tau}} + \bar{x}_{\tau} \quad (20.27)$$

A coastline trader process ends up its life when it is in a profit, that is, to say when $\pi = (\bar{x}_t - a_t^r)e_t \geq \pi_0$, where $\pi_0 = 2\delta/3$ is the profit objective and t is the time expressed in physical time as a position can be in a profit in between events.

Figure 20.6 shows a possible coastline trading scenario. When an overshoot happens, a coastline trader is launched at time 1. With every $+\lambda$ price move, the position grows by an additional $G(1) + G(2)$. If at time 4, the size of the overshoot reduces by one unit, then the exposure is reduced by $G(2)$ units. Note that here, as $\gamma = 1$, the process makes full use of the coastline and minimizes exposure. On the other hand, this setting implies that a stronger price recovery is needed before the position is back in a profit. The trader continues to trade the

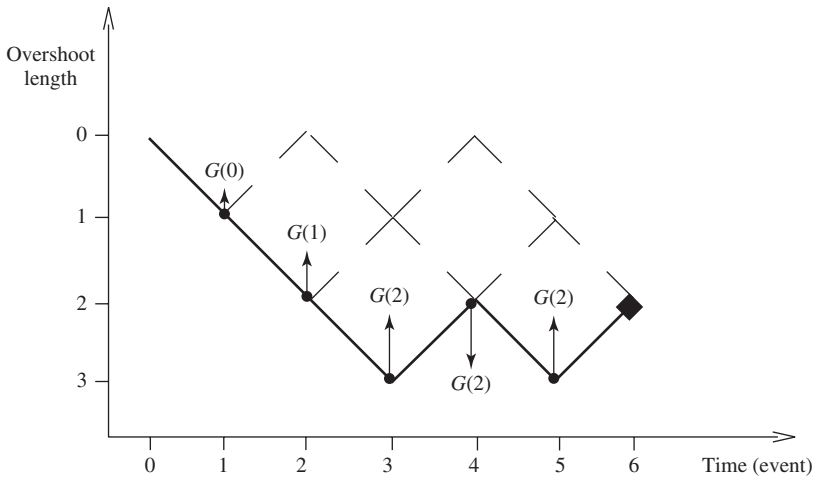


FIGURE 20.6 Occurrence of a coastline investment strategy.

coastline until the position. Then at time 5, the overshoot increases by one unit and the exposure grows by an additional $G(2)$. The exposure is now identical to the one at time 3, but the realized average is smaller. However, in this scenario, the realized average is still not close enough to end the process. Finally, at time 6, the process is terminated and the position is closed, when the profit target has been reached.

20.5.3 MONTHLY STATISTICS

Figure 20.7 shows monthly statistics computed from the execution on a sample account of our investment strategy using coastline trading models, the so-called AF program ols. The trading models of Olsen are based on the above algorithm, and they also include additional risk management mechanisms to manage risk. The running period is 23 months from November 2009 to September 2011 within a portfolio of 24 currency pairs: AUD-CAD, AUD-JPY, AUD-NZD, AUD-USD, CAD-JPY, CHF-JPY, EUR-AUD, EUR-CAD, EUR-CHF, EUR-GBP, EUR-JPY, EUR-NZD, EUR-USD, GBP-AUD, GBP-CAD, GBP-CHF, GBP-JPY, GBP-USD, NZD-CAD, NZD-JPY, NZD-USD, USD-CAD, USD-CHF, and USD-JPY. In Figure 20.7(a), we observe a smoothly increasing cumulated profit that corresponds to the sum of 23 monthly profits for which 16 of them are positive. Figure 20.7(b) shows the distribution of the monthly number of trades summing up to more than 830,000 executed trades. Even though the standard deviation of the sample is large, it is informative to compute the average number of executed trades per minute: $830,000/23/30/24/60 \approx 1$ trade per minute. We observe in Figure 20.7b and c that the trading models react to market activity and provide liquidity when needed. Indeed the lower activity in December 2009 and in the summer of 2010 is due to holidays season. In

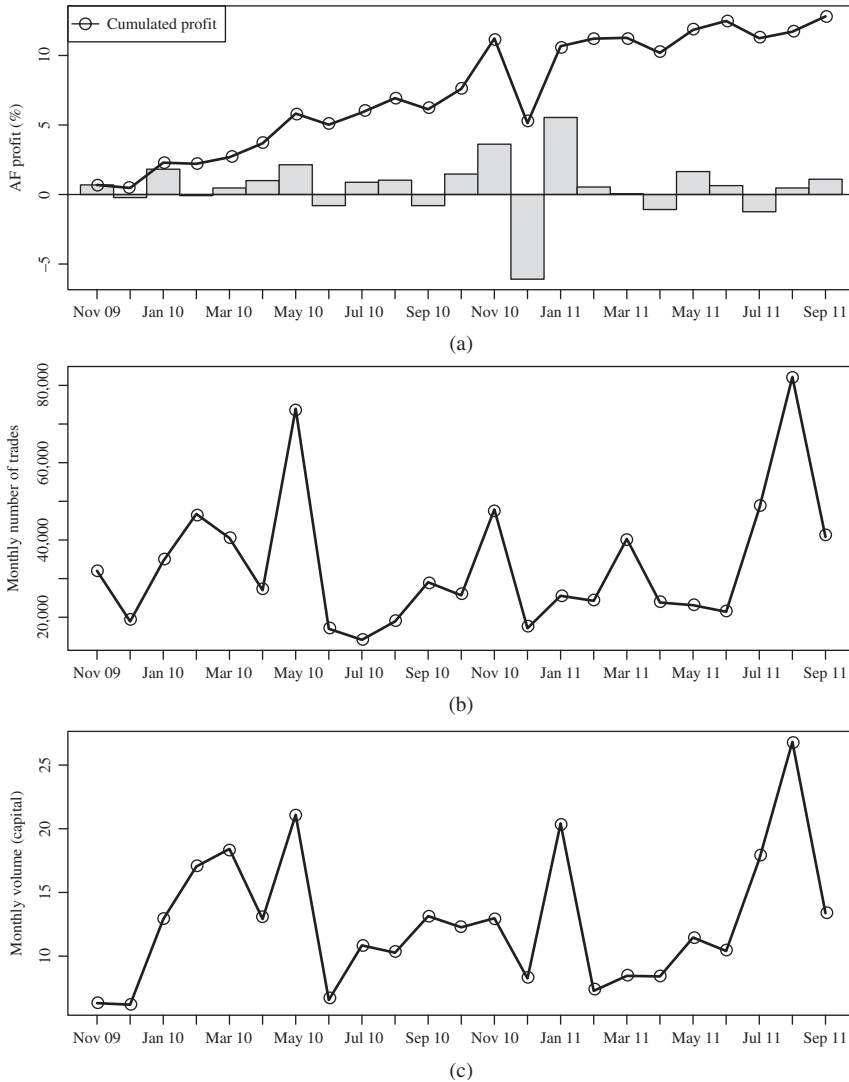


FIGURE 20.7 Monthly statistics of the execution of our trading models on a sample account. Here we show numbers corresponding to the AF program ols. The running period is 23 months from November 2009 to September 2011 within a portfolio of 24 major currency pairs. (a) Bars and the solid line show monthly and cumulated profit, respectively. (b) Monthly number of trades. (c) Monthly volume expressed in multiple of capital. Volume is defined as the sum of the absolute value of executed trades.

contrast, the fairly high activity in May 2010 and August 2011 are, respectively, the result of the flash crash on May 6, 2010, and the CHF approaching parity against the EUR at an extraordinary pace, followed by the SNB establishing a floor in EUR-CHF.

20.6 Conclusion

As we have seen during the current economic crisis, financial markets are unstable. The price instability is a result of demand and supply not balancing each other out for periods of time. We have been able to show that currency markets have distinct statistical properties in the form of scaling laws that have not been discovered before because researchers did not analyze market data using intrinsic time. These properties are useful in several respects. First, it has allowed us to design a SMQ that measures the impact of political and economic events. Second, using the approach of intrinsic time we have shown that it is possible to develop a new class of trading models that balances demand and supply. We have presented an algorithm that generates incremental returns from the long coastline of price moves and inject liquidity into the market, thus contributing to overall market stability and thereby to the overall well-being.

We actually take for granted that these *unexpected* events are bounded, and even more, we assume that they will eventually revert themselves to bounce back where they were. But what if all market participants decide otherwise and all act synchronously as they recently did in the flash crash of May 6, 2010? Should we not have ways to prevent this system from slipping dangerously closer and closer to the precipice? And at the same time generate profit? We believe we should and have partially solved this challenging task by designing high frequency countertrading models providing liquidity when and where it is needed. More work remains to be done and our progress can be followed at www.olseninvest.com.

Acknowledgments

We thank J. B. Glattfelder for discovering the scaling laws and T. Bisig and V. Impagliazzo for designing the Scale of Market Quakes.

REFERENCES

- Balocchi G, Dacorogna MM, Hopman CM, Müller UA, Olsen RB. The intraday multivariate structure of the eurofutures markets. *J Empir Finance* 1999;6:479.
- Barabási A-L, Albert R. Emergence of scaling in random networks. *Science* 1999;286:509.
- Barndorff-Nielsen OE, Prause K. Apparent scaling. *Finance Stoch* 2001;5:103.
- Bauwens L, Hautsch N. Modelling financial high frequency data using point processes. In: Anderson TG, et al., editors. *Handbook of financial time series*. Springer 2009.
- Bisig T, Dupuis A, Impagliazzo V, Olsen RB. The scale of market quakes. *Quant. Finance*. 2012. Reprinted by permission of the publisher (Taylor & Francis), www.tandfonline.com.
- Bouchaud J-P. Power laws in economics and finance: some ideas from physics. *Quant Finance* 2001;1:105.
- Bouchaud J-P. Economics needs a scientific revolution. *Nature* 2009;457:147.

- Bureau of Labor Statistics 2007–2009. Available at www.bls.gov.
- Chaboud A, Chernenko S, Howorka E, Iyer R, Liu D, Wright J. The high-frequency effects of U.S. macroeconomic data releases on prices and trading activity in the global interdealer foreign exchange market. Board of Governors of the Federal Reserve System; Volume 823; 2004.
- Corsi F, Zumbach G, Müller UA, Dacorogna MM. Consistent high-precision volatility from high-frequency data. *Econ Notes Rev Bank Finance Monet Econ* 2001;30:183.
- Dacorogna MM, Gençay R, Müller UA, Olsen RB, Pictet OV. An introduction to high-frequency finance. San Diego (CA): Academic Press; 2001.
- Di Matteo T. Multi-scaling in finance. *Quant Finance* 2007; 7:21.
- Di Matteo T, Aste T, Dacorogna MM. Long term memories of developed and emerging markets: using the scaling analysis to characterize their stage of development. *J Bank Finance* 2005;29:827.
- Dominguez K. The market microstructure of central bank intervention. *J Int Econ* 2003;59:25.
- Engle RF, Ng VK. Measuring and testing the impact of news on volatility. *J Finance* 1993;48:1749.
- Engle RF, Russell JR. Analysis of high frequency financial data. In: Ait-Sahalia Y, Hansen LP, editors. *Handbook of financial econometrics*. 2006. Forthcoming Elsevier.
- Farmer JD, Lillo F. On the origin of power-law tails in price fluctuations. *Quant Finance* 2004;4:C7.
- Gabaix X, Gopikrishnan P, Plerou V, Stanley HE. A theory of power-law distributions in financial market fluctuations. *Nature* 2003;423:267.
- Galluccio S, Caldarelli G, Marsili M, Zhang Y-C. Scaling in currency exchange. *Physica A* 1997;245:423.
- Ghashghaie S, Talkner P, Breyman W, Peinke J, Dodge Y. Turbulent cascades in foreign exchange markets. *Nature* 1996;381:767.
- Glattfelder JB, Dupuis A, Olsen RB. Patterns in high-frequency FX data: Discovery of 12 empirical scaling laws. *Quant Finance* 2010;11:599. Reprinted by permission of the publisher (Taylor & Francis), www.tandfonline.
- Guillaume DM, Dacorogna MM, Davé RD, Müller UA, Olsen RB, Pictet OV. From the bird's eye to the microscope: a survey of new stylized facts of the intra-daily foreign exchange markets. *Finance Stoch* 1997;1:95.
- Joulin A, Lefevre A, Grunberg D, Bouchaud J-P. Stock price jumps: news and volume play a minor role. *Wilmott Mag* 2008. Sept/Oct, 46, 1 (2008).
- Lux T. Financial power laws: empirical evidence, models, and mechanisms. *Economics working papers*; 2006.
- Mandelbrot BB. The variation of certain speculative prices. *J Bus* 1963;36:394.
- Mandelbrot BB, Hudson RL. *The (mis)behavior of markets*. New York: Basic Books; 2004.
- Mantegna RN, Stanley HE. Scaling behavior in the dynamics of an economic index. *Nature* 1995;376:46.
- Müller UA, Dacorogna MM, Olsen RB, Pictet OV, Schwarz M, Morgenege C. Statistical study of foreign exchange rates, empirical evidence of a price change scaling law, and intraday analysis. *J Bank Finance* 1990;14:1189.

- Newman MEJ. Power laws, Pareto distributions and Zipf's law. *Contemp Phys* 2005;46:323.
- Omrane WB, Bauwens L, Giot P. News announcements, market activity and volatility in the euro/dollar foreign exchange market. *J Int Money Finance* 2005;24:1108.
- Richter CF. *Elementary seismology*. San Francisco (CA): Freeman; 1958.
- Sornette D. Fokker-Planck equation of distributions of financial returns and power laws. *Physica A* 2000;290:211.
- Sornette D. *Why stock markets crash: critical events in complex financial systems*. Princeton (NJ): Princeton University Press; 2002.
- West GB, Brown JH, Enquist BJ. A general model for the origin of allometric scaling laws in biology. *Science* 1997;276:122.
- www.olsen.ch.
- www.olseninvest.com.
- www.oanda.com.
- www.ebs.com.
- Zumbach GO, Dacorogna MM, Olsen JL, Olsen RB. Measuring shock in financial markets. *Int J Theor Appl* 2000;3:347.